DESIGN STUDY FOR A SUPERCONDUCTING PROTON LINAC FROM 20 TO 100 MEV*

T. P. Wangler, R. Garnett, F. Krawczyk, J. Billen, N. Bultman,
K. Christensen, W. Fox, and R. Wood
Los Alamos, National Laboratory, Los Alamos, NM 87545

I. INTRODUCTION

Advances in superconducting radiofrequency technology during the past 15 years have made possible the large-scale application of superconducting niobium accelerators. So far this development has been restricted to rather low-current electron and heavy-ion accelerators. In addition to the power savings, the improved capability of superconducting cavities to provide acceleration of high currents with low beam losses, which follows from the ability to use larger beam apertures without a large economic penalty from increased rf losses, could make superconducting proton linacs very attractive for high-intensity applications, where activation of the accelerator is a major concern. During the past year, at Los Alamos, we have been looking at a possible upgrade to the 800-MeV LAMPF proton accelerator, to provide higher intensity injection into a new storage ring for a new high-intensity pulsed neutron source. As part of this upgrade to the LAMPF accelerator, the entire linac below 100 MeV would be rebuilt to provide improved beam quality, improved reliability, and to include funneling at 20 MeV for higher beam currents. Both a room-temperature and a superconducting option are being considered for the section from 20 to 100 MeV. At present, this section is a 201.25 MHz room-temperature copper drift-tube linac (DTL). For this new upgrade scenario the frequency from 20 to 100 MeV was fixed at 805 MHz. The new duty factor is assumed to be 7.2%, and we will show some results at two currents, 30 mA and 150 mA, that span the range of interest. Our superconducting linac concept consists of individual multicell cavities, each driven by a klystrode. Focusing would be provided by superconducting quadrupole lenses between cavities. In the remainder of the paper we describe our study to evaluate the potential of a superconducting proton linac section for this application, and address some of the many design choices.

II. ACCELERATING STRUCTURE STUDIES

Recently, at Argonne, a new niobium accelerating structure, called the spoke resonator[1] has been built and tested at high fields. This structure is suitable for acceleration of high-current beams at the intermediate velocities of interest. This structure is also equivalent to the slotted iris structure that was built many years ago for superconducting applications at Karlsruhe[2]. The cavity that was tested resonated at 855 MHz, and was optimized for a particle velocity of 0.30 c. RF-tests were performed on the cavity and a high accelerating gradient of 7.2 MV/m, limited by magnetic quench, was obtained at a 4.2 K operating temperature. A peak surface electric field of 24 MV/m and a peak surface magnetic field of 560 G were obtained in the cavity. The accelerating gradient achieved in the test is already very attractive for a proton linac application.

For a proton linac it may be more economical to employ accelerating structures with more than two gaps. We have looked at two arrangements for the spokes, a) the ladder geometry where all the spokes are parallel, and b) the cross-bar geometry, where adjacent spokes are rotated by 90 degrees. We have studied the characteristics of both these structures at 805 MHz and at three different velocities, corresponding to 20, 60, and 100 MeV protons, using the 3D electromagnetic code MAFIA(Release 3.1). Figure 1 shows drawings produced by MAFIA for each of these structures. For these initial studies the spoke has been modeled as a rectangular bar of width = 6.0 cm with beveled edges to reduce the peak electric field, and thickness = 0.317 L_c along the axial direction, where $L_c = \beta\lambda/2$ is the cell length, and β and λ are the velocity and rf wavelength. The boundary conditions are defined for MAFIA on the transverse planes that pass through the center of the bars. For the π mode the electric fields are parallel to the boundary
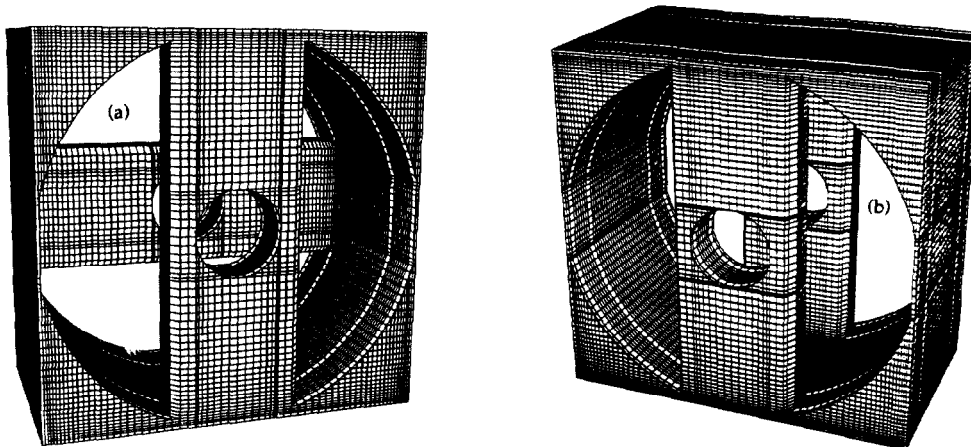

Fig. 1. Views of the multicell cavity structures designed for particles with velocity = 0.428 c produced by MAFIA. a) Cross-bar structure, b) Ladder structure.

plane. The cavity radius R was adjusted until the resonant frequency of the π mode was within 1% of 805 MHz. The results are shown in Table 1, where the cross-bar and ladder structures are designated as CB and L. The notation is: Q_0 is the unloaded quality factor, $R_s(\Omega)$ is the rf surface resistance, T is the transit-time factor, $k = (\omega_\pi - \omega_0)/\omega_{ave}$ is the intercell coupling factor defined in terms of the frequencies of the 0 and π modes, and their average frequency, U(mJ) is the stored energy within a length $\beta\lambda$, E_p(MV/m) is the peak surface electric field, and B_p(mT) is the peak surface magnetic field. The stored energy and field values are normalized so that the accelerating field $E_0T = 1$ MV/m, where E_0 is the spatial average of the axial electric field. The coupling factor k is larger for the CB case but it is probably acceptably large for both structure types.

The peak surface field differences between the two structures are the result of 3D geometry effects. The peak surface electric fields generally occur at the edges of the bar even when the edges are beveled. For the CB structure the electric field lines that originate from the face of a bar tend to terminate preferentially along the edges of the adjacent perpendicular bar, and this concentration produces an enhanced peak surface field. Improvements in the spoke geometry should reduce Ep. The peak surface magnetic field is maximum where the bar intersects the cylindrical wall. For the CB structure the current and the magnetic field are not smoothly distributed around the bar, but are concentrated along the sides. For the CB structure this results in the shortest path for the current. Although the optimization of the geometries is not completed, the smaller peak surface fields for the L structure makes this structure an attractive candidate.

We have also looked at the conventional 0-mode DTL structure. A disadvantage of the 0-mode structure is that the transit-time factor is reduced, because the axial field leaks into the drift tubes, when large apertures are required. We have considered an example in which the drift tubes will not contain a focusing quadrupole, and are designed with noses to compensate for the reduction in the transit-time factor caused by the large aperture. The DTL has been modeled as an azimuthally symmetric structure, and it's properties have been calculated using the 2D electromagnetic code SUPERFISH. The results are also shown in Table 1. By comparison with the spoke-type structures, the DTL also has very strong intercell coupling, lower T, much larger E_p, and smaller B_p (but see footnote for Table 1).

III. BEAM DYNAMICS STUDIES

We present two examples[3] from our study of super-conducting linac solutions using the code CCLDYN. The

multicell cavities are generated for a fixed value of velocity β, all cells in the cavity have the same length $\beta\lambda/2$, and each cavity has a different β. The intertank spaces are chosen to allow adequate room for flanges, bellows, diagnostics, and quadrupole lenses. The beam current, averaged over an rf cycle, is assumed to be either 30 or 150 mA. The accelerating field E_0T as a function of beam energy was obtained from a polynomial fit to MAFIA calculations, and corresponds approximately to a constant peak surface electric field near 20 MV/m. We chose E_0T equal to 3.5 MV/m at 20 MeV, 5.1 MV/m at 60 MeV, and 5.5 MV/m at 100 MeV.

The two linac designs we have considered correspond to a 2.0-cm radial aperture and a fixed energy gain per multicell cavity equal to a) $\Delta W = 1.0$ MeV, and b) $\Delta W = 3.33$ MeV. The number of cells per cavity is determined by ΔW, E_0T, and the synchronous phase. Table 2 summarizes the parameters for the two examples. We interpret the results as follows. For design B the linac is shorter and has fewer components. However, for design B: a) the cavity input power coupler requirements are greater (The present state of the art for input power couplers represents a limit that is generally considered to be about 100 kW.), and b) the transverse aperture-to-rms beam size ratio is lower as a result of the reduced transverse phase advance per focusing period, leading to a larger beam envelope and indicating increased beam-loss potential. We consider that for 150 mA the transverse aperture to rms ratio is probably more than adequate for design A, and the longitudinal ratio is more than adequate for design B. In these designs with quadrupoles between all cavities, increasing the cavity energy gain and length increases the quadrupole period, which for fixed 80° transverse phase-advance per period, reduces the overall quadrupole focusing strength. However, it improves the overall longitudinal focusing, because of the reduced number of intertank spaces. The beam dynamics optimum in cavity energy gain lies somewhere between the two designs. Additional optimization would include the choices of aperture and synchronous phase.

It may be desireable from the point of view of reliability to restrict the number of gaps per cavity to only 2 or 3, so that failure of a single cavity would result in only a minor perturbation on the overall linac performance. We have not had time to explore this issue, but we note that the multicell cavities for the two designs presented here could be replaced by groups of two or three gap cavities. Thebeam dynamics results for this case should be similar to what has

Table 1 MAFIA results for cross-bar(CB) and ladder(L) structures in the π mode and DTL structure in 0 mode.

Type	β	R(m)	$Q_0R_s(\Omega)$	T	k	U(mJ)	E_p(MV/m)	B_p(mT)*
CB	0.207	0.0745	63.7	0.782	0.58	16.9	6.16	24.9
CB	0.341	0.0845	85.0	0.776	0.46	17.6	4.14	16.4
CB	0.428	0.0891	93.3	0.771	0.40	21.4	3.86	14.6
L	0.207	0.0981	62.5	0.782	0.31	18.8	5.09	19.4
L	0.341	0.1000	86.5	0.777	0.30	18.3	3.58	13.6
L	0.428	0.1003	93.9	0.779	0.30	21.0	3.43	13.0
DTL	0.207	0.10	207.9	0.498	0.90	23.6	20.5	8.16
DTL	0.341	0.10	213.6	0.641	0.61	23.2	14.4	7.20
DTL	0.428	0.10	210.1	0.633	0.51	32.0	14.2	8.09

* For the DTL this does not include the factor of 2 stem enhancement.

Table 2 Comparison of 805 MHz, 20-100 MeV Superconducting Linac Designs

PARAMETER	DESIGN A	DESIGN B
Energy gain per cavity (MeV)	1.00	3.33
E_0T (MV/m)	3.5 to 5.5	3.5 to 5.5
Synchronous Phase (deg)	-40 to -35,	-40
Cells per Cavity	9 to 3	30 to 9
Number of Cavities	87	26
Cavity Lengths (m)	0.18 to 0.36	0.71 to 1.18
Cavity Input Power (kW)	30 (30 mA)	100 (30 mA)
	150 (150 mA)	500 (150 mA)
Intercavity Spacing	5.5 $\beta\lambda$ to 3.5 $\beta\lambda$	5.5 $\beta\lambda$ to 3.5 $\beta\lambda$
Aperture Radius(cm)	2.0	2.0
Transverse Aperture to Rms Beam-Size Ratio	14-25 (30 mA)	7-14 (30 mA)
	11-19(150 mA)	6-10 (150 mA)
Longitudinal Aperture to Rms Beam-Size Ratio	6-9 (30 mA)	12-13 (30 mA)
	5-6 (150 mA)	10-11(150 mA)
Focusing Lattice Type	Doublet	Doublet
Total Length(m)	62.0	36.9

been already presented in this paper, provided that the gaps required between cavities are small.

In Table 3 we show various power values at operating temperatures of both 2K and 4.2K. The peak rf power of 2.4 MW is determined by the beam power for an assumed 30 mA beam current. The average rf power is obtained by applying the 7.2% duty factor. The rf surface resistances are taken from measurements at 805 MHz on single-cell niobium elliptical cavities[4] at Ep= 20 MV/m, and the surface resistance at 2K is lower than at 4.2K by a factor of 16.7. The rf power dissipation in the niobium structure has been obtained by using the parameters from the MAFIA calculations for the L structure. The static heat leak is estimated[5] at 7 W/m of cryostat length, and the length is taken from the design A value of 62 m. Because the static heat leak is a continuous load, while the rf load is pulsed, the static effect is dominant at 2K and is comparable to the rf load at 4.2K. For this reason the large temperature dependence in the rf surface resistance does not produce a correspondingly large difference in the thermal power into the Helium. The refrigeration-efficiency[6] difference favors the 4.2K temperature, mostly because of the temperature dependence of the Carnot efficiency factor. The net result is that the ac refrigeration power is about equal for the two operating temperatures. This conclusion would change in favor of 2K operation, if the accelerating field increased, if the duty factor increased, or if the static heat load decreased.

Table 3 Superconducting Linac Power Values

Operating Temperature	2K	4.2K
Beam current (mA)	30	30
Peak rf power(MW)	2.4	2.4
Average rf power (kW)	170	170
Niobium rf surface resistance (nΩ)	24	400
Peak rf power-niobium (W)	520	8600
Average rf power-niobium(W)	37	620
Static heat leak power (W)	430	430
Total power into Helium(W)	470	1050
Refrigeration efficiency	1/1200	1/530
AC power for refrigeration(kW)	560	560
AC klystrode power(kW)	370	370
Total ac power (kW)	930	930

The ac power for the klystrodes is calculated using an efficiency factor[7] of 47%. The final conclusion is that at 30 mA the peak rf power required is 2.4 MW, and the total ac operating power (refrigeration plus klystrodes) is just under 1 MW. The superconducting linac sections would reduce the peak rf power by 7.0 MW and the ac operating power by 0.8 MW, compared to the existing 201.25 MHz room-temperature copper DTL.

IV. ACKNOWLEDGMENTS

VI. REFERENCES:

[1] J. R. Delayen, W. L. Kennedy, and C. T. Roche, "Design and Test of a Superconducting Structure for High-Velocity Ions", Proceedings of the 1992 Linear Accelerator Conference, Ottawa, Ontario, Canada, 24-28 August, 1992, AECL Report AECL-10728, p 695.

[2] K. Mittag, "Superconducting Accelerator Structures for Medium Energy Protons", IEEE Trans. Nucl. Sci., Vol. NS-24, No. 3, 1156 (1977).

[3] R. W. Garnett, "Example Beam Dynamics Solutions for a 20-100 MeV Superconducting Linac for LANSCE-II", Los Alamos Accelerator Technology Division Technical Note No. AT-1:93-099, April 15, 1993.

[4] Brian Rusnak, Los Alamos, private communication.

[5] C. H. Rhode and D. Proch, "Cryogenic Operation for Cavity Systems", Proc. of 4th Workshop on RF Superconductivity, KEK Report 89-21, KEK Laboratory, Tsukuba, Japan, August 14-18, 1989, p 751.

[6] P. Lebrun, "Cryogenic Systems", Superconductivity in Particle Accelerators< CERN Accelerator School Proceedings, CERN 89-04, Hamburg, Germany, May 30-June 3, 1988, p 66.

[7] Mike Lynch, Los Alamos, private communication.